Nanotechnology Perceptions
ISSN 1660-6795
www.nano-*ntp.com*

First-Principles Calculations Of Structural, Electronic, And Optical Properties Of Spinel Zn_2MO_4 (M= Ti, Si, Pb)

Saad Boudabia [1], Ahmed Draoui [2,3], Yamina Benkrima [4]

[1] *Laboratoire de Mathématique et sciences appliquées, LMSA Université de Ghardaïa, Algeria.*
[2] *Laboratoire de Physique des Matériaux (LPM), Université Amar Telidji de Laghouat, Algeria.*
[3] *Laboratoire de sciences chimiques et physiques appliquées, école normale supérieure de Laghouat, Algeria.*
[4] *Ecole Normale Supérieure de Ouargla 30000, Algeria.*
Email: boudabia.saad@univ-ghardaia.edu.dz

Received: 12/09/2024 ; Accepted: 27/12/2024

In the present study, we investigate first-principles calculations to determine the structural, electronic and optical properties of spinel-type oxides Zn_2MO_4 (M = Ti, Si, Pd) using the pseudo-potential plane wave method within density functional theory (DFT), as implemented in the BIOVIA Material Studio and the CASTEP code. This study aims to evaluate the optical properties of three spinels with identical crystalline structures under ambient conditions and determine which is best suited for optoelectronic applications. We began by proving their mechanical stability, then calculated their gap energy, as this is closely related to their optical properties. The exchange and correlation functionals used are generalized gradient approximation with the Perdew-Burke-Ernzerhof (GGA-PBEsol), for structural and mechanical properties. The results obtained show that there is a good analogy with previous studies and also that Zn_2TiO_4 with its semiconductor behavior (a moderate gap Eg=3.33 eV) and its high absorption in the UV-visible range makes it the best candidate for opto-electronic applications.

Keywords: Spinel, DFT calculation, Band structure, Density of states (DOS) and Optical properties.

Introduction

AB_2O_4 is the generic formula for spinel oxides, a class of mixed metal oxides in which A and B are usually metal cations that occupy different crystallographic positions inside a cubic close-packed oxygen framework. This structure, which was first discovered in the mineral spinel ($MgAlO_4$) [1], is incredibly adaptable and can incorporate a variety of metal ions, which adds to its remarkable chemical flexibility and vast range of functional uses. Oxygen anions give spinel oxides their face-centered cubic (fcc) structure, with trivalent B-site cations

occupying octahedral sites and divalent A-site cations occupying tetrahedral sites. Spinels are categorized as normal ($(A)_{tet}[B_2]_{oct}O_4$), inverted ($(B)_{tet}[A\ B]_{oct}O_4$), or mixed ($(A_{1-x}B_x)_{tet}[A_xB_{2-x}]_{oct}O_4$ Where $0<x<1$) varieties based on the configuration of cations between these sites [2]. Numerous electrical, magnetic, and catalytic characteristics are displayed by spinel oxides. These result from significant electron–electron correlations in some transition metal-based spinels as well as the interaction of cation size, charge, and distribution. Spinel's usefulness in contemporary materials research is further increased by the capacity to modify its characteristics through cation replacement, doping, or nanostructuring [3-4]. Notably, the spinel is extensively utilized in multiple fields due to its advantageous physical, structural, electronic, and optical properties [5-6]. Recent studies indicate that incorporating different dopants can significantly alter the electronic band structure, enhancing its suitability for semiconductor applications [7]. Moreover, its high refractive index and low dispersion make it ideal for optical devices [8]. The material shows strong catalytic properties, particularly for environmental remediation and energy conversion, due to its effective charge transfer processes essential for catalytic activity [9]. Research into spinel-type oxides is driving innovation across various industries, highlighting their crucial role in modern technology [10]. As researchers explore the complexities of these materials, new applications and enhancements are expected to emerge, further establishing their significance in advanced ceramics [11].

This study focuses on spinel Zn_2MO_4 (M = Ti, Si, Pd), which has a closed-packed face-centred cubic structure, classified under space group Fd-3m (number 227). In this structure, Zn ions occupy 8a tetrahedral sites, M ions are found in 16d octahedral sites, and O ions reside in 32e sites Fig.1 [12]. The lattice parameter a_0 characterizes these compounds, which are analyzed using ab initio computations to determine their structural, electronic, and optical properties [13].

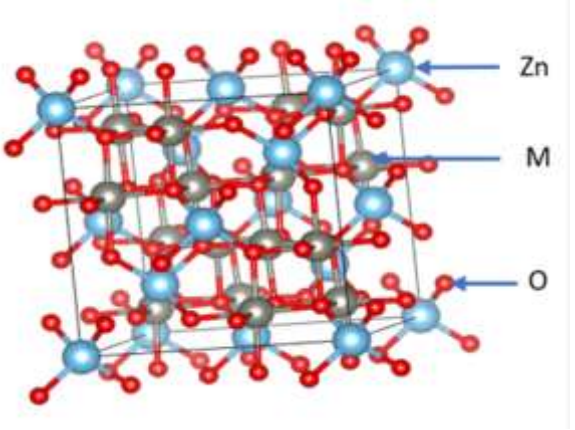

Fig. 1: Zn_2MO_4 Crystal structure.

1. Computational methods:

Essential physical properties have been calculated using the pseudo-potential plane wave method within density functional theory (DFT), as implemented in the BIOVIA Material

Studio [14] and the CASTEP module [15]. The generalized gradient approximation with the Perdew-Burke-Ernzerhof functional (GGA-PBEsol) was applied for exchange-correlation interactions. A Vanderbilt-type ultrasoft pseudopotential was employed with the following electronic configurations:
Zn ($2p^6$,$3p^6$,$3d^{10}$), Si ($2p^6$,$3p^2$), Ti ($2p^6$,$3p^6$,$3d^2$), and Pb ($2p^6$,$3p^6$,$3d^{10}$,$4d^{10}$).
To ensure convergence and achieve precise results a, 7 × 7 × 7 Monkhorst-Pack mesh was used for k-point integrations over the Brillouin zone for all compounds, with a kinetic energy cut-off set at 500 eV. The structural parameter a_0 was determined using the Broyden-Fletcher-Goldfarb-Shanno optimization technique [16-19].

2. Results and discussion

1.1. Structural properties

The unit-cell parameters and the bulk modulus at zero pressure of the three materials were initially calculated after optimization and then compared with experimental and theoretical results. These results are presented in Table 1. The unit-cell of Zn_2TiO_4 calculated in the present study align closely with both experimental results and some previous theoretical studies.

Table 1: Calculated lattice parameter a_0(Å), bulk modulus B_0(GPa) for Zn_2MO_4 (M = Ti, Si, Pd) with experimental data and other theoretical results.

Materials	Zn_2TiO_4		Zn_2SiO_4		Zn_2PdO_4	
	a_0 (A°)	B_0 (GPa)	a_0 (A°)	B_0 (GPa)	a_0 (A°)	B_0(GPa)
Present study	8.435	170.672	5.820	177.887	6.065	160.337
Other work	8.522 [20] 8.440 [21]	162.9 [25]	8.075 [23]	222.2 [23]	-------	-------
Experimental	8.472 [22]	162.0 [26]	……..	……	8.509 [24]	-------

The present study also shows that Zn_2PdO_4 is more compressible than Zn_2TiO_4 and Zn_2SiO_4 because its bulk modulus is the smallest. This is because the atomic mass of Pd is the largest. Consideration of the mechanical stability of materials was introduced by Born and Huang [27], who demonstrated that, for a crystal, it is possible to formulate stability criteria as a function of elastic constants. For cubic structures, the generalized mechanical stability conditions are expressed as follows:

$$\begin{cases} C_{11} > 0, C_{44} > 0 \\ C_{11} - C_{12} > 0 \\ C_{11} + 2C_{12} > 0 \end{cases} \quad (1)$$

In consideration of the values calculated for the elastic constants in Table 2, and following the application of the established criteria, it is evident that all materials examined in this study exhibit mechanical stability.

Table 2: Calculated elastic constants in GPa for Zn_2MO_4 (M = Ti, Si, Pd).

Materials	Zn_2TiO_4	Zn_2SiO_4	Zn_2PdO_4
C_{11}	**224.32085**	**243.5924**	**208.9540**
C_{12}	**143.8482**	**135,0350**	**136.0288**
C_{44}	**75.0171**	**98.6681**	**53.3468**

1.2. Electronic properties

Analysis of the electronic characteristics of Zn_2MO_4 spinels (M=Ti, Si, and Pd) is essential to understand their possible optical properties. First-principles calculations, using density functional theory (DFT), have been carried out on all three materials to determine, in particular, their band structures and densities of states (DOS).

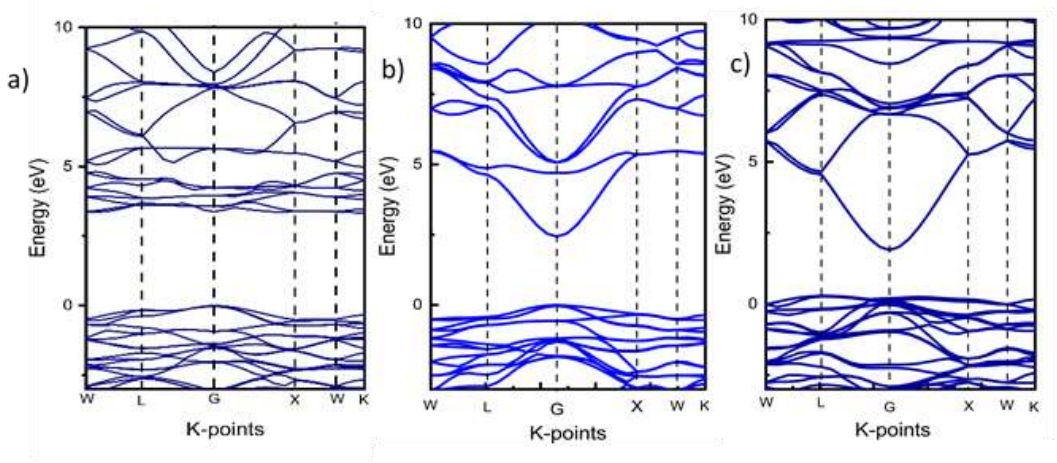

Fig. 2: Band structures of Zn_2MO_4 . a) Zn_2TiO_4, b) Zn_2SiO_4, and c) Zn_2PdO_4.

A. Band structure

The band structures of Zn_2TiO_4 and Zn_2SiO_4, as illustrated in Fig 2.a and 2.b, respectively, show that the valence band maximum and the conduction band minimum are both located at the same Gamma point of the Brillouin zone, indicating direct transitions or direct gaps. In the case of Zn_2PdO_4, however, the valence band maximum is located at the L point and the conduction band minimum is at the Gamma point of the Brillouin zone, presenting an indirect

L-Gamma gap, as illustrated Fig 2c. The bandgap values of the three materials are illustrated and compared with other theoretical results in Table 3.
The band structures further reveal the dominance of the valence bands by the O-2p and Zn-3d hybrid states, while the conduction bands are dominated by the Ti-3d states for Zn_2TiO_4, Si-3p for Zn_2TiO_4, and Pd-4d for Zn_2PdO_4.

Table 3: Calculated band gap $E_g(eV)$ for Zn_2MO_4 (M = Ti, Si, Pd) with experimental data and other theoretical results.

Materials	Present study	Other work	Experimental
	Band gap Eg(eV)		
$\mathbf{Zn_2TiO_4}$	3.335	2.660[a]	3.100 [b]
$\mathbf{Zn_2SiO_4}$	2.432	2.780[c]	4.360 [c,*]
$\mathbf{Zn_2PdO_4}$	1.610	-----	------

a: Ref [20]
b: Ref [28]
c: Ref [29]

*: The divergence between the theoretical and experimental values is due to the fact that the LDA and GGA functionals underestimate the gap energy.

B. Density Of States (DOS)

Fig 3 illustrates the partial state densities of the three materials, with a marked evolution of electronic properties through this series of materials. Zn_2SiO_4 in Fig 3.b, shows a typical semiconductor structure, characterized by dominant O-2p/Zn-3d hybridization in the valence band (-10 to 0 eV) and conduction states mainly associated with Si-3p. The PDOS in Fig 3.a, that of Zn_2TiO_4 which shows intermediate behavior, with more marked Ti-3d/O-2p hybridization and a significant density of states at the Fermi level suggesting semi-metallic properties. However, in Fig 3.c, Zn_2PdO_4 shows a markedly different electronic structure, with pronounced Pd-4d/O-2p hybridization at -3.5 eV, a significant density of states at the Fermi level confirming its metallic character, and conduction states dominated by Pd-4d (intense peak at 2.5 eV). This progression - from semiconducting (Zn_2SiO_4) to metallic (Zn_2PdO_4) - can be explained by the evolution of orbital contributions: while Zn_2SiO_4 is dominated by covalent Si-O interactions, Zn_2PdO_4 shows a more metallic character due to Pd-4d states. However, all three materials share a significant hybridization between O-2p and metallic states (Zn-3d, Ti-3d or Pd-4d), and it is this hybridization that determines their optical properties and thermochemical stability. These differences in electronic structures suggest distinct applications: Zn_2SiO_4 for optoelectronics, Zn_2TiO_4 for photocatalytic applications, and Zn_2PdO_4 as a conductive material or catalyst.

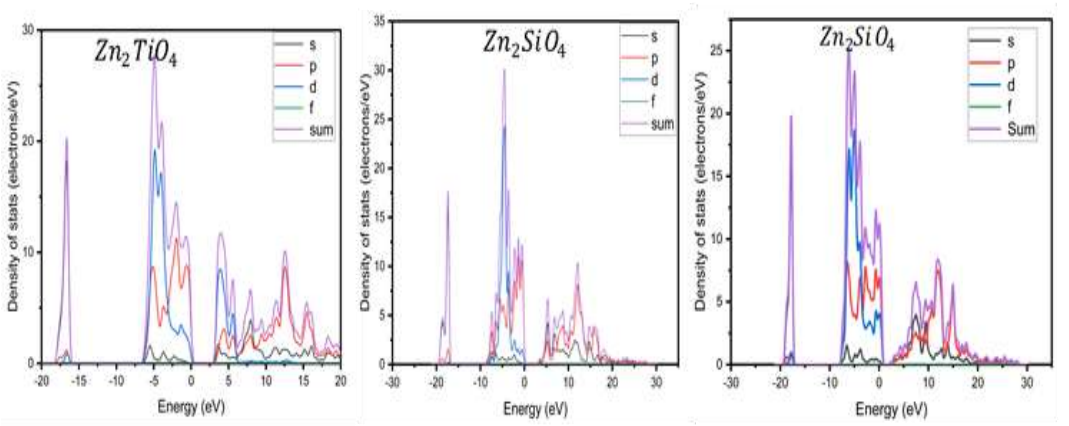

Fig. 3: Partial Density of States of Zn_2MO_4. a) Zn_2TiO_4, b) Zn_2SiO_4, and c) Zn_2PdO_4.

1.3. Optical properties

A more thorough analysis of the graphs shown in Fig 4 reveals distinct optical properties in all three spinels. Zn_2TiO_4 demonstrates semiconductor characteristics, exhibiting a fundamental band gap of approximately 3.3 eV, which is indicative of an absorption peak in $\varepsilon_2(\omega)$ at 4.8 eV and moderate reflectivity (<25% in the visible). In contrast, Zn_2SiO_4, which is a wide bandgap insulator, shows a negligible absorption in the visible and high transparency with low reflectivity (<10%). However, Zn_2PdO_4 manifests metallic properties, as indicated by its high reflectivity (>70% in the infrared-visible) and significant UV absorption.

Consequently, Zn_2TiO_4 and Zn_2SiO_4 exhibit selective UV absorption and differ in their band gaps, while Zn_2PdO_4 is clearly distinguished by its metallic behavior. Given its optical properties, Zn_2TiO_4 is regarded as the most promising candidate for optoelectronic applications, surpassing Zn_2SiO_4 and Zn_2PdO_4 in this regard. Its moderate bandgap is optimal for efficient absorption in the near-UV range (3-5eV), making it particularly suitable for photodetection applications. Furthermore, the high absorption of Zn_2TiO_4 around 4.8 eV positions it as a premier material for active optoelectronics applications.

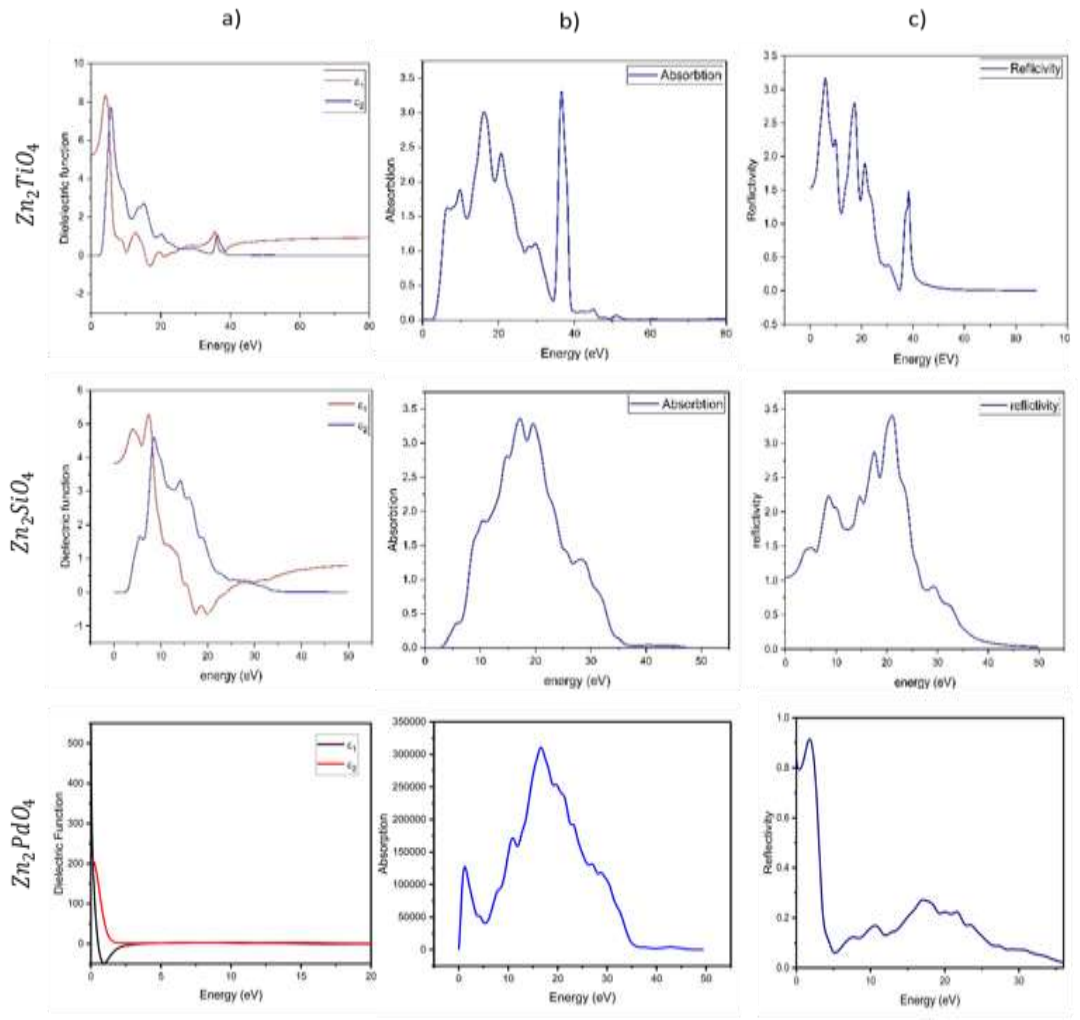

Fig. 4: Optical parameters of Zn_2MO_4 (M=Ti, Si, Pd). a) Dielectric function b) Absorption, and c) Reflectivity.

2. Conclusion

First-principles calculations were carried out to determine and compare the structural, electronic, and optical properties of Zn_2TiO_4, Zn_2SiO_4, and Zn_2PdO_4. The materials analyzed in this study demonstrate robust mechanical stability. The analysis of the real part of the dielectric function revealed a significant agreement in the gap energy between the experimental result and our results, at least for Zn_2TiO_4. The evolution of the imaginary part of the dielectric function indicates a strong absorption in the UV energy spectrum and part of the visible spectrum of the same compound. In the basis of these results, we intend to make this material the subject of a future study in order to use it for the development of a photovoltaic cell.

References

[1] Zhao, Q., Yan, Z., Chen, C., & Chen, J. (2017). Spinels: controlled preparation, oxygen reduction/evolution reaction application, and beyond. Chemical reviews, 117(15), 10121-10211.
[2] Restrepo, O. A., Arnache, Ó., & Mousseau, N. (2024). An approach to understanding the formation mechanism of NiFe2O4 inverse spinel. Materialia, 33, 102031..
[3] Tavakolipour, R., Pournajaf, R., & Grazenaite, E. (2024). Synthesis and doping of high-temperature resistant spinel nano pigments: A review.
[4] Fakhry, F., Shaheen, E., El-Dosoky, H., Meaz, T. M., Mubark, M., & El-Shater, R. (2024). Elastic and magnetic characteristics of nano-spinel ferrite Co0. 5 MgxCu0. 5− xFe2O4. Scientific Reports, 14(1), 29407.
[5] Draoui, A., Hebboul, Z., Lefkaier, I. K., & Naidjate, M. E. (2022). Facile synthesis route and characterizations of zinc orthotitanate nanoparticles tested for dye-sensitized solar cell DSSC applications. Journal of the Iranian Chemical Society, 19(11), 4515-4522.
[6] Sickafus, K. E., Wills, J. M., & Grimes, N. W. (1999). Structure of spinel. Journal of the American Ceramic Society, 82(12), 3279-3292.
[7] Zhou, Y., Sun, S., Song, J., Xi, S., Chen, B., Du, Y., ... & Xu, Z. J. (2018). Enlarged Co□ O Covalency in Octahedral Sites Leading to Highly Efficient Spinel Oxides for Oxygen Evolution Reaction. Advanced Materials, 30(32), 1802912.
[8] Shannon, R. D., & Rossman, G. R. (1992). Dielectric constants of silicate garnets and the oxide additivity rule. American Mineralogist, 77(1-2), 94-100.
[9] Vozniuk, O., Tabanelli, T., Tanchoux, N., Millet, J. M. M., Albonetti, S., Di Renzo, F., & Cavani, F. (2018). Mixed-oxide catalysts with spinel structure for the valorization of biomass: The chemical-loop reforming of bioethanol. Catalysts, 8(8), 332.
[10] Bhaskar, A., Mikhailova, D., Kiziltas-Yavuz, N., Nikolowski, K., Oswald, S., Bramnik, N. N., & Ehrenberg, H. (2014). 3d-Transition metal doped spinels as high-voltage cathode materials for rechargeable lithium-ion batteries. Progress in Solid State Chemistry, 42(4), 128-148.
[11] Deka Boruah, B., Mathieson, A., Park, S. K., Zhang, X., Wen, B., Tan, L., ... & De Volder, M. (2021). Vanadium dioxide cathodes for high-rate photo-rechargeable zinc-ion batteries. Advanced Energy Materials, 11(13), 2100115.
[12] Wyckoff, R. W. G., & Wyckoff, R. W. (1963). Crystal structures (Vol. 1, pp. 239-239). New York: Interscience publishers.
[13] Blaha, P., Schwarz, K., Tran, F., Laskowski, R., Madsen, G. K., & Marks, L. D. (2020). WIEN2k: An APW+ lo program for calculating the properties of solids. The Journal of chemical physics, 152(7).
[14] Dassault Systèmes (2023), BIOVIA Materials Studio [Logiciel]. San Diego, CA : Dassault Systèmes.
[15] Clark, S. J., Segall, M. D., Pickard, C. J., Hasnip, P. J., Probert, M. I., Refson, K., & Payne, M. C. (2005). First principles methods using CASTEP. Zeitschrift für kristallographie-crystalline materials, 220(5-6), 567-570.
[16] Broyden, C. G. (1970). The convergence of a class of double-rank minimization algorithms 1. general considerations. IMA Journal of Applied Mathematics, 6(1), 76-90.
[17] Fletcher, R. (1970). A new approach to variable metric algorithms. The computer journal, 13(3), 317-322.
[18] Goldfarb, D. (1970). A family of variable-metric methods derived by variational means. Mathematics of computation, 24(109), 23-26.
[19] Shanno, D. F. (1970). Conditioning of quasi-Newton methods for function minimization. Mathematics of computation, 24(111), 647-656.
[20] Xiao, L. P., Zeng, L., & Yang, X. (2019). Electronic and optical properties of spinel Zn 2 TiO 4 under pressure effect: ab initio study. The European Physical Journal B, 92, 1-6.

[21] Matsumoto, Y., Omae, M., Watanabe, I., & Sato, E. I. (1986). Photoelectrochemical properties of the Zn-Ti-Fe spinel oxides. Journal of The Electrochemical Society, 133(4), 711.
[22] Zhang, Y., Liu, X., Shieh, S. R., Bao, X., Xie, T., Wang, F., ... & Prakapenka, V. B. (2017). Spinel and post-spinel phase assemblages in Zn 2 TiO 4 : an experimental and theoretical study. Physics and Chemistry of Minerals, 44, 109-123.
[23] Karazhanov, S. Z., Ravindran, P., Vajeeston, P., Ulyashin, A. G., Fjellvåg, H., & Svensson, B. G. (2009). Phase stability and pressure-induced structural transitions at zero temperature inZnSiO3 andZn2SiO4. Journal of Physics: Condensed Matter, 21(48), 485801.
[24] Demazeau, G., Omeran, I., Pouchard, M., & Hagenmuller, P. (1976). Sur une nouvelle phase oxygenee du palladium+ IV: Zn2PdO4. Materials Research Bulletin, 11(11), 1449-1452.
[25] Zhang, Y., Liu, X., Shieh, S. R., Bao, X., Xie, T., Wang, F., ... & Prakapenka, V. B. (2017). Spinel and post-spinel phase assemblages in Zn 2 TiO 4: an experimental and theoretical study. Physics and Chemistry of Minerals, 44, 109-123.
[26] Wang, Z., Saxena, S. K., & Zha, C. S. (2002). In situ X-ray diffraction and Raman spectroscopy of pressure-induced phase transformation in spinel Zn 2 TiO 4. Physical Review B, 66(2), 024103.
[27] Born, M., & Huang, K. (1988). Dynamical Theory of Crystal Lattices Oxford Classic Texts in the Physical Sciences, Clarendon.
[28] Matsumoto, Y. (1996). Energy positions of oxide semiconductors and photocatalysis with iron complex oxides. Journal of solid state chemistry, 126(2), 227-234.
[29] Karazhanov, S. Z., Ravindran, P., Fjellvåg, H., & Svensson, B. G. (2009). Electronic structure and optical properties of ZnSiO3 and Zn2SiO4. Journal of Applied Physics, 106(12).